TECHNICAL MEMORANDUM

431

Simulation of the yield and accuracy of wind profile measurements from the Atmospheric Dynamics Mission (ADM-Aeolus).

David G.H. Tan and Erik Andersson

Research Department

Submitted to Q. J. R. Meteorol. Soc.

January 2004

European Centre for Medium-Range Weather Forecasts
Europäisches Zentrum für mittelfristige Wettervorhersage
Centre européen pour les prévisions météorologiques à moyen terme

Series: ECMWF Technical Memoranda

A full list of ECMWF Publications can be found on our web site under:
http://www.ecmwf.int/publications/

Contact: library@ecmwf.int

European Centre for Medium Range Weather Forecasts
Shinfield Park, Reading, RG2 9AX, England

Abstract

The European Space Agency's ADM-Aeolus mission will for the first time provide wind profile measurements from space. In this study we carry out global simulations to predict the yield and accuracy of future ADM-Aeolus wind profile measurements, using realistic clouds and climatological aerosol distributions. Based on an assessment of wind analysis accuracy we argue that the main Aeolus impacts are to be expected (1) in the jet streams over the oceans, especially away from main air traffic routes, and in the African/Asian subtropical jet; (2) in the lower troposphere, e.g. western parts of the N. Pacific and N. Atlantic oceans and the Mediterranean, if cloud gaps are sufficient, and (3) in the tropics, where mass-wind balance is weak and hence temperature information is not effective for inferring wind. These expectations are supported by the simulations of the yield and accuracy of ADM-Aeolus data. Observational data from the LITE campaign in 1994 are used to provide realistic profiles of cloud cover as input to such simulations. Profiles of model cloud cover are also used and these are validated against the LITE data. While the overall occurrence of model cloud agress well with LITE-inferred cloud, model cloud cover underestimates the observations by around 20%. The use of model cloud cover for simulating Aeolus data thus results in a modest overestimation of Aeolus penetration altitude. Probability distributions of Aeolus instrument error show good agreement between simulations with observed and model cloud, but the worst 10% of errors are underestimated when model cloud cover is used. Overall, the yield and accuracy of simulated Aeolus data are high and compare favourably with radiosondes, with more than 90% of data meeting accuracy requirements in the free troposphere (errors below 2 ms^{-1}). At low altitudes, two thirds of data from the Mie channel meet accuracy requirements (errors below 1 ms^{-1}) even when substantial cloud is encountered.

Contents

1 Introduction

The Atmospheric Dynamics Mission (ADM-Aeolus) is the second of ESA's Earth Explorer Core Missions [ESA, 1999]. Its objective is to demonstrate the capability to measure wind profiles from space using a Doppler Wind Lidar (DWL). The ADM is designed to provide high-quality wind profiles from the surface up to 20 km [Stoffelen *et al.*, submitted]. In the atmosphere's baroclinic regions, the need for good vertical resolution data and the prevalence of cloud pose severe challenges for the global observing system. Active remote sensing by lidars can potentially meet both these challenges, thereby overcoming intrinsic limitations of passive remote sensing techniques. In this study we carry out global simulations to predict the yield and accuracy of future ADM-Aeolus wind profile measurements, using realistic clouds and climatological aerosol distributions.

The DWL will provide layer averaged wind measurements with a 1000 m vertical resolution through most of the atmosphere (i.e. from 2 to 16 km), 500 m below 2 km, and 2000 m between 16 and 20 km (Fig. 1). There is information on the horizontal line-of-sight (HLOS) wind component only. The schematic in Fig. 1 shows the instrument viewing from a low-altitude ($\sim$ 400 km) polar orbit in the direction perpendicular to the satellite track. The DWL is the only instrument onboard the ADM platform. It is scheduled for launch in October 2007 and has a projected lifetime of three years. The mission requirements with respect to observation acccuracy have been developed to meet scientific goals of user communities in climate research, atmospheric modelling and Numerical Weather Prediction (NWP) [ESA, 1999]. Meteorological observations, particularly those with well-understood and quantified error characteristics, are an essential component of NWP. Data assimilation procedures use the available observations to derive atmospheric analyses (estimates of the atmospheric state). Higher-quality observations are required to improve the accuracy of analyses and associated forecasts. Profile measurements in meteorologically sensitive regions [Buizza and Montani, 1999] are a priority because these regions have high baroclinicity and thus play an important role in the development and intensification of weather systems [Browning *et al.*, 2000].

The accuracy of the ADM wind measurements will depend primarily on the intensity of the backscattered laser light, which in turn depends on the presence and thickness of clouds, and the concentration of aerosol. It is expected that sufficient backscatter will be received from the layers of clear air above clouds, from cloud-top layers, from layers in and below thin clouds, and from layers with sufficient aerosol in the lower parts of the atmosphere. In the current study we investigate the yield and accuracy of ADM wind profiles through detailed simulations, given realistic cloud distributions and climatological estimates of aerosol concentration. In particular we aim to answer the question: To what extent can the ADM instrument deliver high quality wind data in meteorologically sensitive regions with significant cloudiness?

The simulations in this study rely on the provision of realistic cloud cover, cloud water content and on accurate modelling of laser backscatter intensity in clear-sky and cloudy conditions. We use cloud data generated by the Autumn-2002 version of the ECMWF atmospheric model at full horizontal resolution (T511). Simulated backscatter is calculated using the LIPAS (LIdar Performance Analysis Simulator) forward model, developed specifically for the ADM lidar [Veldman *et al.*, 1999, Stoffelen *et al.*, 2002]. The realism of the simulated backscatter has been verified against actual space-borne lidar backscatter measurements available from the LITE mission [McCormick *et al.*, 1993, Winker *et al.*, 1996] on the American Space Shuttle in September 1994, provided consistent aerosol backscatter coefficients are employed [Marseille *et al.*, submitted]. We assess the quality of the model clouds against cloud retrievals, also obtained from the LITE data set.

In the following section we indicate the regions where the main benefit of ADM data should be expected. We review the current availability of wind data for global NWP applications and present an estimate of current wind analysis accuracy. So-called "key analysis errors" [Klinker *et al.*, 1998] are presented in order to identify the sensitive regions. In Section 3 we describe the LITE data set, the LIPAS simulator and the methodology used in the present study. Section 4 is devoted to a validation of model clouds against LITE-data cloud retrievals.

The results from simulations of the yield and accuracy of ADM wind-profile measurements are presented in Section 5. Section 6 contains conclusions and recommendations for future work.

2 Available wind observations for NWP, and estimates of wind analysis accuracy

In this section we review the current availability of wind observations for global NWP, and provide indication of the regions where the main benefit of ADM data should be expected.

2.1 Current availability of wind observations for global NWP

The ECMWF data assimilation system currently makes use of more than 1.5 million meteorological observations per 12-hour assimilation cycle [Thépaut and Andersson, 2003]. The model atmospheric state has many more degrees of freedom ($\sim 10^7$) and some aspects of the analysis problem remain under-determined ([Fisher, 2003]). The analysis accuracy in the less well-observed regions depends on the accuracy of the assimilating forecast model and the predictablility of the atmosphere. The radiosonde network provides *in situ* observations of wind, temperature and humidity. These are arguably the most valuable source of wind profile information but coverage over ocean regions is poor. Remotely sensed data consist primarily of radiance observations from passive instruments. The vertical resolution of such data is typically several kilometres, which is inadequate for many important meteorological situations. In addition, infrared sounders are unable to observe below clouds. Radiance observations are most useful for the information they provide on the temperature (hence mass) and humidity fields of the atmosphere. For large-scale dynamics, balance relationships are invoked to infer wind information from the temperature information provided by the radiance observations. However, these relationships have limited ability to infer wind information for the tropics ([Žagar *et al.*, submitted]), where Coriolis forces are weak, and for smaller-scale extra-tropical dynamics, e..g. storms and fronts, with horizontal scales of 100–1000 km and vertical scales less than a few kilometres.

Other types of wind data are available at a limited number of vertical levels. Wind speed at the ocean surface can be inferred from remotely sensed scatterometer data, through relationships between surface wind speed and ocean capillary waves ([Isaksen and Janssen, submitted]). Tracking of features in cloud imagery can yield atmospheric motion vectors ([Schmetz *et al.*, 1993]) but is subject to errors in height assignment. Wind data from commercial aircraft [Cardinali *et al.*, 2003] are abundant at the main cruise altitudes of flight tracks. The profile information available from aircraft ascents and descents is concentrated around airports, so the coverage is far less than what is required for global data assimilation. An active area of current research is the exploitation of observations of other meteorological quantities such as cloud cover and precipitation, which may offer some indirect improvement for wind analyses, particularly in the tropics.

In summary, the most important and most challenging requirement for global meteorological analysis remains the observation of wind profiles with high accuracy, global coverage, and good vertical resolution [WMO, 2001]. In the remainder of this section we present examples of wind errors in analyses and short-range forecasts that make use of currently available meteorological observations. These examples are chosen to substantiate the points made above concerning the regions and spatial scales where better wind data are most needed.

2.2 Estimates of wind errors in global analyses and short-range forecasts

Estimates of wind errors in analyses and short-range forecasts can be obtained through several different means. These include:

- Theoretical error estimates produced by the data assimilation procedure [Fisher and Courtier, 1995],
- Statistics of observation-minus-background differences (innovations, departures) and observation-minus-analysis differences (residuals) [Hollingsworth and Lönnberg, 1986],
- The amplitude and structure of "key analysis errors" [Klinker *et al.*, 1998],
- The spread of a data assimilation ensemble, in which random noise is added to all observations used [Fisher and Andersson, 2001].

Here we will use the latter two approaches to illustrate the main areas where better wind observations are required.

Key analysis errors are the perturbations to meteorological analyses that give most improvement to 48-hour forecasts [Klinker *et al.*, 1998]. They are based on the adjoint sensitivity of 48-hour forecast error with respect to the forecast's initial condition (the analysis) [Rabier *et al.*, 1996]. The method assumes that all of the 48-hour forecast error can be attributed to errors in the initial condition (i.e. zero model error) and that the tangent-linear assumption is valid over the 48-hour range. Climatologies of key analysis errors have been calculated by e.g. [Marseille and Bouttier, 2001] and used as indication of the atmosphere's sensitive regions where additional observations would be most valuable. Key analysis errors have only been computed routinely at ECMWF since 1998, using the adjoint of the linearized forecast model. Because this paper focusses on the LITE period in 1994, we computed the r.m.s. of key analysis errors for the period 9–16 September 1994, based on recent analyses described Section 4.2.

At 250 hPa (Figure 2) the largest perturbations are found in the jet stream regions, especially over the oceans. At 850 hPa (Figure 3, left panel), the North Atlantic and North Pacific storm tracks feature prominently. The perturbations are small in amplitude, around 0.5 m/s, but grow rapidly through baroclinic instability mechanisms. Baroclinic instability is largely responsible for the highly tilted structures and small vertical scales evident in key analysis perturbations. Small-scale mixing and condensation processes are also associated with the storm tracks, and result in substantial cloud cover (Figure3, right panel). Much of this cloud occurs at high altitudes, limiting the effectiveness of passive infrared temperature and humidity sounding [McNally, 2002]. DWL has the potential to yield useful data here, all the way down to the cloud top layer, below thin clouds and in gaps between clouds. Indeed, the purpose of our study is to quantify the frequency and accuracy of ADM data in sensitive and cloudy regions.

Figure 4 shows an example of ensemble spread for zonal wind accuracy at 250 hPa. The assimilation ensemble [Fisher and Andersson, 2001] comprises 10 members, each run for 31 days of October 2000 using the Autumn-2001 version of the ECMWF forecast system (labeled 23r4). The rms difference of the 12-hour forecasts is shown, and illustrates the main features of short-range forecast uncertainty. These same uncertainties are comparable to the background errors employed in data assimilation, and hence provide some guidance with respect to user requirements for observation errors in new systems such as ADM-Aeolus. The largest uncertainties, exceeding 4 ms^{-1}, are found in the tropics, over the oceans in the Southern Hemisphere, as well as in the Northern Hemisphere storm track regions away from the main air-traffic routes. The large values in the tropics coincide with the areas of strong convective rainfall along the inter-tropical convergence zone. Elsewhere, values exceeding 1.5 ms^{-1} are typical. The advent of ATOVS data has yielded significant reductions in Southern

Hemisphere analysis uncertainty [Simmons and Hollingsworth, 2002], but there remains a general lack of wind data there.

2.3 Discussion

We conclude this section by anticipating developments in Aeolus timeframe (2007–2010). The storm track regions in both hemispheres are highly baroclinic and DWL is one of the few observing systems that promises the vertical resolution (1 km) required to observe important flow structures in these regions. Data from high-resolution passive sounding instruments (e.g. IASI on the European METOP platform) will increase but fundamental problems in infrared sounding in the presence of cloud will persist. Thus, the main Aeolus impacts are to be expected

- in the jet streams over the oceans, especially away from main air traffic routes, and in the African/Asian subtropical jet;
- in the lower troposphere in e.g. western parts of the North Pacific and North Atlantic oceans and the Mediterranean, if cloud gaps are sufficient.
- in the tropics, where mass-wind balance is weak and hence temperature information is not effective for inferring wind.

3 Methodology, and description of used data sets and software

It is expected that the accuracy of the ADM doppler winds will depend directly on the intensity of the backscattered laser light at the receiver. The signal-to-noise ratio is higher the more photons have been received and detected. This is dependent on instrument characteristics as well as the atmospheric conditions ([Marseille and Stoffelen, 2003]). The molecular (Rayleigh) backscatter depends on the air pressure, and attenuation by clouds. The aerosol (Mie) backscatter depends on aerosol concentration, presence of clouds and the optical properties of clouds. There can also be a weak dependency on temperature. To estimate the accuracy of ADM winds we therefore need to simulate the instrument itself, the atmospherc conditions and the effects on the laser beam due to clouds and aerosols. We rely on the LIPAS software (described below) to simulate the ADM instrument and the atmospheric backscatter. We use the ECMWF forecast model at full operational resolution to simulate the atmosphere and clouds. Aerosol distributions are taken from climate.

As both clouds and aerosols are uncertain we verify aspects of the simulation against actual space borne lidar data. For this purpose we have used data from the LITE instrument flown on the American Space Shuttle for a 10-day period (9–18 September) in 1994.

3.1 The LIPAS ADM-Aeolus simulator

This study makes extensive use of simulated ADM-Aeolus data obtained from LIPAS (LIdar Performance Analysis Simulator) [Veldman *et al.*, 1999, Stoffelen *et al.*, 2002]. It simulates the performance of spaceborne Doppler wind lidars, including Aeolus' current baseline instrument [Stoffelen *et al.*, submitted]: a laser operating at 355 *nm*, with separate Mie and Rayleigh direct-detection receiver channels for returns from aerosol/cloud and molecules, respectively ([Marseille and Stoffelen, 2003]). The user specifies parameters such as the observation resolution, shot-accumulation length and pulse repetition frequency.

Aeolus instrument performance parameters (see Table 2 of [Marseille and Stoffelen, 2003]) have been updated following current (September 2002) baseline assumptions as advised by ESA/ESTEC. A 1 km accumulation length is now used (was 3.5 km), telescope diameter is set to 1.5 m (was 1.1 m) and the instrument's optical performance has been reduced slightly. Pending the Preliminary Design Review other parameters are still confidential and subject to change, but are considered conservative.

Various sources of instrument error (random and systematic) are modelled according to industry specifications. Other biases, e.g. laser pointing errors and height assignment errors arising from non-uniform aerosol distributions, are now modelled by LIPAS but were not available in earlier ADM studies, e.g. the Observing System Simulation Experiments (OSSE) by [Stoffelen and Marseille, 1998, Marseille *et al.*, 2001].

Several assumptions potentially affect the realism of LIPAS simulation of Aeolus data. Cloud profiles are assumed constant over a horizontal accumulation length (1 km) but vary within a single observation ($\sim$ 50 km) assuming maximum-random overlap (same as in the ECMWF forecast model [Jakob and Klein, 2000]). Droplet size is assumed to vary linearly with pressure (same as in ECMWF forecast model until January 2002). No distinction is made between backscatter from liquid cloud and ice cloud. The shape and size of ice crystals affect multiple scattering and hence backscatter signal strength [Chepfer *et al.*, 1999] but the uncertainties are comparable to uncertainties in choice of backscatter-to-extinction ratio. The climatological aerosol backscatter profiles are assumed to have no horizontal variability. A constant backscatter-to-extinction ratio is assumed, the precise value being specified by the user (0.02 sr^{-1} has been used in previous studies and is retained here).

The main outputs from LIPAS are simulated Aeolus observations at user-specified resolution, together with profiles of estimated random, systematic and representativeness error. LIPAS provides estimates of ADM observation accuracy as a sum of observation error and representativity error variances. The representativity error is calculated for a reference model grid length of 50 km (Note 100 km was used in some earlier ADM studies). Two representativity errors are calculated: σ_{P50} for a "point" HLOS observation, which can be regarded as one wind component from a "perfect" radiosonde, i.e. one for which there is no instrument error and only representativity error; and σ_{50} for the Aeolus HLOS observation. In the following, random error arising from instrument effects is denoted by $\hat{\sigma}_M$ and $\hat{\sigma}_R$ for the Mie and Rayleigh channels respectively, and the corresponding Aeolus observation random errors are defined as $\sigma_M = (\sigma_{50}^2 + \hat{\sigma}_M^2)^{1/2}$ and $\sigma_R = (\sigma_{50}^2 + \hat{\sigma}_R^2)^{1/2}$. The ratios of Aeolus observation random error to point representativity error, σ_M/σ_{P50} and σ_R/σ_{P50}, are classified as very good, good, poor or very poor if they fall in the range 0–0.9, 0.9–1.8, 1.8–2.7, 2.7–∞, respectively.

3.2 Clouds and aerosol

The main meteorological inputs required for ADM simulation are profiles of wind, temperature, humidity, cloud cover, cloud liquid water content and cloud ice water content. These are obtained from the atmospheric model of the ECMWF forecasting system. Aerosol concentration is another critical input of the simulations, which, however, cannot be obtained from current NWP models. Lipas provides several options: (i) select from the "Vaughan climatology" [Vaughan *et al.*, 1995, Veldman *et al.*, 1999], 5 climatological profiles derived from measurement campaigns at 10.6 μm over the Atlantic during the relatively clean atmospheric period 1988-1990, (ii) use the mean and standard deviation from the climatology to produce random, spatially uncorrelated, realizations of aerosol backscatter, or (iii) select from the "LITE4ADM climatology", 10 climatological profiles derived for the LITE period [Marseille *et al.*, submitted]. The LITE4ADM profiles imply around 5 times more aerosol backscatter than the Vaughan climatology in the upper troposphere and lower stratosphere because of the presence of aerosol from the 1991 Mt. Pinatubo eruption.

We make extensive use of ECMWF model cloud cover fields. These have been validated against radiance observations, and have well-known deficiencies such as a systematic lack of stratocumulus cloud off the west coast of

the continents [Chevallier *et al.*, 2001] and limited success in capturing the observed temporal variability in the intertropical convergence zone (ITCZ) [Chevallier and Kelly, 2002]. While these studies do not provide much guidance on the impact such deficiencies have on Aeolus simulations, the LITE mission [Winker *et al.*, 1996] provides useful independent data to assess the reasonableness of Aeolus modelling assumptions. Consequently, we have chosen to assess the yield and accuracy of simulated Aeolus data in the LITE period 9–18 September 1994. The sensitivity of the simulations with respect to deficiencies in the assumed cloud cover has been assessed (Section 4).

3.3 The LITE data set

We validate the ECMWF model cloud cover using LITE data from 65 orbits comprising 12389 profiles of cloud cover. The LITE-inferred cloud cover available at ECMWF was derived elsewhere in two steps. First, a cloud-boundary detection algorithm adapted from [Winker and Vaughan, 1994] was applied to raw LITE data from the 532 and 1064 nm channels. Second, the cloud-boundary information was converted to cloud cover at 1 degree horizontal resolution and 31 vertical levels [Miller *et al.*, 1999], corresponding to ECMWF's former operational model. (Note that [Miller *et al.*, 1999] use the term "pseudo-cloud fraction" for the cloud cover product).

It is difficult to quantify the accuracy of the LITE cloud cover product. The thresholds used in the cloud detection were high in the sense that, excluding clouds located underneath dense clouds, any cloud missed would be extremely tenuous (optical depth less than 0.005 say). Subvisible cirrus (optical depth less than 0.03) accounts for around 5–10% of inferred cloud cover [Winker, personal communication]. [Miller *et al.*, 1999] remark that pulse stretching could lead to an underestimation of cloud base altitude and hence an overestimation of low-level cloud cover.

4 Lidar sensitivity to temperature and aerosols, and Validation of model clouds

Before we proceed with the simulation of ADM wind measurement accuracy we investigate the sensitivity of lidar photon counts with respect to aerosol concentration, and carry out a validation of model cloud cover.

4.1 Lidar (photon count) sensitivity to temperature and aerosol

In the simplest model of the Doppler wind lidar observation principle, the HLOS wind component is directly proportional to the shift in frequency between the transmitted photons and the received photons. The quality of an observation depends on the instrument signal-to-noise ratio, which in turn depends on the amplitude of the backscattered signals, i.e. the *number* of received photons. Figure 5 shows photon count sensitivity to different temperature and aerosol backscatter profiles. The temperature profiles are typical zonal mean profiles for Northern Hemisphere winter (ECMWF operational model, January 2002). The effect of lower temperature is to increase molecular density which results in more molecular backscatter and hence slightly improved signal quality in the DWL Rayleigh channel. However, photon counts exhibit far greater sensitivity to the assumed aerosol backscatter profile. The five profiles from the Vaughan climatology (see Sec. 3.1) vary by an order of magnitude at any given altitude and over several orders of magnitude vertically. While four profiles vary monotonically with height and give photon counts that increase with increasing aerosol backscatter, the upper decile profile has a layer of enhanced aerosol backscatter around 10 km. The corresponding photon counts are large from the top of this layer, but substantial attenuation occurs so that, below 8 km, the received signal is much weaker than for the monotonic aerosol profiles. The contrast in observation quality is shown in Figure 6

for the median and upper decile aerosol backscatter profiles. Better quality is obtained from the aerosol layer at 10 km and virtually no useful data between 0 and 1 km due to strong attenuation. In the case of the upper decile aerosol profile, better quality is also obtained between 2 and 6 km. This is an example in which the aerosol backscatter is sufficiently strong to increase the yield and accuracy of data from the Mie channel, outweighing the degraded quality in the Rayleigh channel. It follows that the specification of aerosol and cloud backscatter warrants careful consideration.

In the near future, further valuable data on aerosol and cloud backscatter variability can be expected from satellite missions such as ICESat and Calipso. If successful, these missions will provide profile information that is not available from e.g. MODIS, which nonetheless is providing useful information on horizontal variability of aerosol. In the following our simulations have been performed with the Vaughan median profile. In terms of random errors, simulations with higher aerosol loadings indicate that better performance from the Mie channel outweighs Rayleigh channel degradation. Simulated systematic errors with the median profile are virtually identical to previous estimates [ESA, 1999], e.g. 0.84 ms^{-1} for the Mie channel at 2 km, 1.3 ms^{-1} for the Rayleigh channel at 10 km.

4.2 Validation of model cloud cover

A necessary preparation for this study has been to derive high resolution meteorology for the LITE period in 1994. Previous model fields available for this period are inadequate because of insufficient resolution. By re-running the period with the curent version of the ECMWF forecasting system we take avantage of recent improvements in physical and dynamical aspects of the model. In addition, the ERA-40 re-analysis project [Uppala, 1997] has provided better knowledge on how to use the observational data available at that time. We have therefore applied a recent version of the operational model at full resolution (cycle 25r1, 40 km grid, 60 levels) to the LITE period in 1994, assimilating all the observations available in ERA-40 to produce the best posssible analyses and forecasts. Relative to ERA-40 assimilations, Cy25r1 uses an improved version of the RTTOV radiative transfer scheme, so new bias corrections for HIRS and SSM/I radiance observations had to be generated and employed. The forecast fields from the model have been archived every 2 hours. For comparison with LITE data, these fields are sampled at the time within the range T+12 to T+36 that is closest to the actual orbit overpasses.

We have compared the model cloud fields with LITE cloud retrievals. As an example, Figure 7 shows cloud cover inferred from LITE observations for orbit 047 and from the ECMWF model. The current model has 60 vertical levels so these have been reduced for the purposes of the present comparison to 31 levels which approximately coincide with the LITE cloud product. Where levels have been merged, the maximum-random cloud overlap assumption has been applied [Jakob and Klein, 2000].

Qualitatively, the main features in Figure 7 and similar plots of several other LITE orbits are:

- The occurrence of model cloud cover shows fairly good agreement with LITE-inferred cloud cover. Cloud top height agrees quite well.
- Model cloud cover underestimates LITE-inferred cloud cover by 20% on average. Note that LITE in essence samples each model grid box along a narrow one-dimensional slice. In the context of nadir-pointing cloud radar, analogous sampling issues lead to comparable biases [Astin, 1997].
- The model has a systematic lack of low-level cloud. While accurate modelling of stratocumulus cloud is an acknowledged difficulty, discrepancies with LITE may be exaggerated by the effects of pulse stretching (see Section 3.3).

Due to the model's systematic lack of low-level clouds and other uncertainties in cloud amounts and cloud properties, we decided to perform two sets of ADM simulations: with model clouds and with LITE-inferred clouds. Results were compared in terms of simulated backscatter and wind measurement accuracy.

5 Yield and accuracy of simulated Aeolus data in the LITE period

We assess simulated Aeolus data produced from the meteorology of the LITE-period assimilation as described above. The simulated data are compared with a reference simulation, in which model cloud cover is replaced by LITE-inferred cloud cover. We show the comparison when the assumed aerosol backscatter is given by the Vaughan median profile. It is for this comparatively low atmsopheric aerosol loading that sensitivity to the assumed cloud cover is most apparent.

5.1 Sensitivity to cloud cover for low aerosol loading

Figure 8 shows the percentages of simulated mid-latitude Aeolus data for which the ratio σ_A/σ_{P50} falls into the ranges 0–0.9, 0.9–1.8, 1.8–2.7, 2.7–∞, where $\sigma_A = \min(\sigma_M, \sigma_R)$, i.e. the better of the two simulated wind observations from the Mie and Rayleigh channels is chosen. The simulations in the upper and lower panels assume model cloud cover and LITE-inferred cloud cover, respectively. Overall the correspondence is good. The simulated data based on model cloud cover overestimate the percentage of "very good" quality (ratio less than 0.9) and underestimate the percentage of "very poor" quality (ratio more than 2.7). This is consistent with the model underestimation of cloud cover. The discrepancies in quality are most pronounced in the layers between 0–2 km where the use of model cloud cover underestimates very poor quality data by some 25%. Above 3 km, the percentage of very good data (ratio less than 0.9) is overestimated when model cloud cover is used but the discrepancy is no more than 10%. It should be noted that the poor data are easily identifiable through their poor signal-to-noise ratio and can be removed from further processing by the users of future ADM data. The indentification of poor data thus affects the yield rather than the accuracy of the final product.

As an alternative measure of Aeolus yield, consider the penetration altitude of Aeolus data. We apply a demanding definition, namely the altitude below which more than 10% of simulated data are classified as very poor. With model cloud cover the penetration altitude is 4 km in mid-latitudes. This is more optimistic than the penetration altitude associated with LITE-inferred cloud cover (5 km, Figure8, upper and lower panels). It should be noted that with this particular definition of penetration altitude as much as 70% of data below that level remain good.

Aeolus performance has also been examined for the subtropics and the tropics (plots not shown). In comparison to the mid-latitudes, the most significant feature of tropical performance is that Mie channel detection of scattering from cirrus cloud results in 15–20% of Aeolus data being classified as very good between 12 and 16 km. The simulated transmission through thin cirrus remains high so there is no major degradation in quality at lower altitudes. As for mid-latitudes, the results are robust to whether the cloud cover field is Lite-inferred or from the ECMWF model. Even with LITE-inferred cloud cover, the percentage of very poor data between 0 and 2 km is smaller in the subtropics and tropics than in the mid-latitudes (15–30% rather than 20–40%). With LITE-inferred cloud cover, 20% of tropical data below 6 km are very poor but, as for mid-latitudes, this penetration altitude is overestimated with model cloud cover (just 10% very poor down to 0 km.)

5.2 Instrument random error profiles

Another perspective on Aeolus performance is provided by examining the probability distributions of simulated Aeolus instrument random error, $\hat{\sigma}_R$ and $\hat{\sigma}_M$ for the Rayleigh and Mie channels respectively. Such distributions contain more detail than the four ranges used for quality classification and are of interest for the quality control aspects of data assimilation, for example. The upper panel in Figure 9 shows the instrument error distribution for the Aeolus Rayleigh channel as a function of altitude. The thick solid curve connects the median error at each altitude and thus represents a "typical" error profile. The spread of the distribution at each level is shown by horizontal lines: solid lines connect the lower and upper quartiles, dashed lines the lower and upper deciles. Above 9 km, cloud effects are small and compact error distributions for the Rayleigh channel are evident. The reduction in errors above 16 km is associated with the change in vertical resolution from 1 km to 2 km. With decreasing altitude, clouds degrade the amplitude of returned lidar signals and result in skewed error distributions with greater probability of large errors. However, median errors decrease with decreasing height (due to increasing molecular density) until around 2 km where attenuation in the Rayleigh channel is too strong.

For reference, the thick dash-dot curve shows the Aeolus mission requirements. These are met comfortably by large amounts of Rayleigh channel data: more than 90% between 9 and 12 km, more than 75% between 4 and 9 km. It can be seen that the Rayleigh channel median error exceeds the mission requirements around 2 km. Conversely, the Mie channel (Figure 9, lower panel) performs well below 2 km, with median errors less than 0.2 ms^{-1} and almost 75% of all data complying with the mission specification. Median errors in the Mie channel increase sharply above 2 km, exceeding 5 ms^{-1} above 3 km. Nonetheless, the best 10% of Mie channel returns between 2 and 13 km are below 0.2 ms^{-1}. These are due to scattering in cloud tops. Such cloud top returns may yet prove valuable, but further research is required to assess their representativeness.

5.3 Observation random error profiles

To assess the usefulness of Aeolus data in an operational data assimilation environment, it is relevant to examine observation random errors σ_R and σ_M (Figure 10). Because they combine instrument error and representativity error, these observation errors are inversely proportional to the weight that would be given to isolated observations in data assimilation procedures. They are thus directly comparable to the observation error assigned to radiosonde wind observations, in the ECMWF system. The ECMWF radiosonde obervation errors are shown for reference as the thick dashed curve. Taking the Rayleigh channel above 2 km and the Mie channel below, the median observation random errors for Aeolus compare favourably with radiosondes. At many altitudes, the Aeolus upper quartile and upper decile are better than radiosondes, implying a high yield.

We can corroborate the findings of Section 2 by showing the distributions of Mie channel observation random error in the mid-latitudes and in particular the North Atlantic. Recall that use of model cloud cover results in overestimation of Aeolus data quality. This is manifested in Figure 11, upper panel, by the compact error distribution between 0 and 1.5 km, 90% of errors are below 1.6 ms^{-1}. By constrast, LITE-inferred cloud cover results in more skewed error distributions (lower panel) with around 25% of errors exceeding 1.7 ms^{-1}. A similar increase in skewness is evident in the Rayleigh channel (figure not shown), but the effect is only noticeable in the upper decile. For example, at 4.5 km in the North Atlantic, use of model cloud cover in place of LITE cloud cover changes the Rayleigh channel upper decile observation error from 2.7 ms^{-1} to 4 ms^{-1}. The remainder of the error distribution is remarkably robust, with the corresponding changes in lower decile, median, and quartiles all being less than 1%.

	Domain N/W/S/E	Rayleigh		Mie		
		4–5 km	9–10 km	0.5–1 km	4–5 km	9–10 km
N.Hem	90/-180/20/180	75	93	70	16	22
Tropics	20/-180/-20/180	77	87	71	11	18
S.Hem	-20/-180/-90/180	82	99	59	17	15
N.Atl	65/-70/25/-10	72	92	63	17	27
N.Pac	60/145/25/-130	69	91	57	15	23
E.Asia	60/102.5/25/150	64	93	50	25	26
ITCZ	20/80/0/-80	56	70	62	10	38
S.Atl	-30/-60/-55/60	75	98	59	15	24
S.Pac	-20/-180/-45/-90	83	97	53	19	15

Table 1: Percentage of data meeting mission accuracy requirements.

5.4 Geographical distribution of yield and cloudiness

To assess the geographical distribution of expected Aeolus yield, simulated Aeolus data have been grouped in 5 degree by 5 degree bins. Within each bin, the percentage of simulated data that meet the mission accuracy requirements is calculated. The results are shown in Figures 12, 13 and 14 for altitude ranges 9–10 km, 4–5 km and 0.5–1 km respectively. To relate the performance of the Rayleigh and Mie channels to the cloud cover encountered, the three figures also show r.m.s. of high, medium and low cloud cover (shaded). Contrary to future real ADM data, our simulated data are co-located with LITE cloud cover profiles and hence are confined to 60S–60N. There are also no LITE data available between 60–80E.

Rayleigh channel yield for 9–10 km exceeds 75% (green markers) throughout most of the extratropics (Figure 12, upper panel). High cloud over the North Atlantic and the Southern Hemisphere oceans does not reduce yield significantly at this altitude. In the Tropics, areas of high cloud cover, specifically the ITCZ and the West Pacific warm pool, correlate with reduced Rayleigh channel yield (70%). Conversely, good Mie channel yield relies on the presence of cloud (Figure 12, lower panel) at this high altitude.

Figure 13 shows yield at 4–5 km. The Rayleigh channel is still good in cloud-free regions. There is however a systematic reduction in yield in regions where the DWL must penetrate high cloud – see Table 1. For example, Rayleigh channel yield in the North Atlantic is 92% at 9–10 km, reducing to 72% at 4–5 km. In the ITCZ, the corresponding change is from 70% to 56%. Mie channel yield is still linked to the presence of cloud, and complements the Rayleigh channel.

At 0.5–1 km, the Rayleigh channel yields no data that meet the mission requirements. The Mie channel however is expected to perform well when scattering from cloud tops is strong, and this is confirmed e.g. off the west coasts of the continents where stratocumulus cloud is prevalent, as well in the Southern hemisphere storm tracks. Aeosol returns are also expected to yield good Mie channel data at this altitude, and would explain the high yield in cloud-free regions.

6 Conclusions and future work

Provision of high-quality observations of the global wind field remains an important objective for advancing numerical weather prediction. In Section 2 we have shown typical wind uncertainties in the ECMWF forecast system, reflecting in part the deficiencies in the current global observing system. The observation requirements

defined for the Aeolus mission suggest that the data should significantly improve NWP. In providing wind profiles with high vertical resolution, Aeolus is expected to improve analyses

- in the jet streams over the oceans, especially away from main air traffic routes, and in the African/Asian subtropical jet;
- in the lower troposphere, e.g. western parts of the N. Pacific and N. Atlantic oceans and the Mediterranean, if cloud gaps are sufficient,
- in the tropics.

The results in Section 5 support these expectations. Simulated Rayleigh channel yield at 9–10 km typically exceeds 90%. The ITCZ is a noteworthy exception, where reduced Rayleigh channel yield is complemented by 38% Mie channel yield. At 4–5 km, Rayleigh channel yield ranges from 56 to 83% for the regions examined in Table 1. The corresponding range for the Mie channel is 10–25%. At 0.5–1 km, simulated Mie channel yield is in the range 50–71%.

Our simulations of Aeolus measurement accuracy are found to be robust to large variations in cloud cover, thus reducing previous uncertainties in anticipated performance. Aeolus observation errors compare favourably with the errors assigned to radiosonde wind observations in an operational weather prediction environment. This provides further evidence that, by meeting the mission observation requirements as currently specified, significant impact of ADM-Aeolus winds can be expected in NWP.

In Section 4 we also assessed the impact of different cloud cover assumptions on simulated Aeolus data. The study focussed on the period 9–18 September 1994. We compared the yield and accuracy of simulated Aeolus data for two cloud cover scenarios: cloud cover is specified either by ECMWF model fields or by a cloud cover product derived from observations made during the Lidar In-space Technology Experiment (LITE). Although model fields underestimate the LITE-inferred cloud cover by 20% on average, Aeolus yield and accuracy under the two scenarios show good agreement in several measures. This is an encouraging result because future simulations and planned impact assessment studies will rely heavily on model cloud cover fields. Overestimation of the penetration altitude of Aeolus does arise when model fields are used, but the effect is relatively small. Discrepancies are generally confined to the tails of error distributions. Nevertheless, this needs to be taken into account in future work, particularly in developing quality control thresholds.

We note that in the current simulations, the limits on yield and accuracy may be affected by the fact that each simulated observation over 50 km horizontally is the simple arithmetic average of fifty 1 km accumulations. If there is sufficient cloud variability within such accumulations, it may be possible to increase yield and accuracy by more selective averaging procedures. We recommend that this aspect be given due attention in the development of ADM data processing software, and in future simulations.

Acknowledgements

We thank Ad Stoffelen and Gert-Jan Marseille for assistance with LIPAS, Steve Miller, Dave Winker and Frederic Chevallier for assistance with LITE-inferred cloud cover and members of ESA's ADM mission advisory group for valuable comments and suggestions. We are also grateful to our colleagues within ECMWF's Data Assimilation Section for help and useful discussions, especially Lars Isaksen and Carla Cardinali with own experience from earlier ADM simulations. The study was funded under ESA contract No. 15342/01/NL/MM.

References

[Astin, 1997] Astin, I., 1997: Sampling errors and bias in satellite-derived fractional cloud cover estimates from exponential and deterministic cloud fields as a consequence of instrument pixel size and number. *J. Atmos. Oceanic. Technol.*, **14,** 1146–1156.

[Buizza and Montani, 1999] Buizza, R. and A. Montani, 1999: Targeting observations using singular vectors. *J. Atmos. Sci.*, **56,** 2965–2985.

[Browning *et al.*, 2000] Browning, K. A., A. J. Thorpe, A. Montani, D. Parsons, M. Griffiths, P. Panag and E. M. Dicks, 2000: Interactions of tropopause depressions with an extropical cyclone and sensitivity of forecasts to analysis errors. *Mon. Wea. Rev.*, **128,** 2734–2755.

[Cardinali *et al.*, 2003] Cardinali, C., L. Isaksen and E. Andersson, 2003: Use and impact of automated aircraft data in a global 4D-Var data assimilation system. *Mon. Wea. Rev.*, **131,** 1865-1877.

[Chevallier *et al.*, 2001] Chevallier, F., P. Bauer, G. Kelly, C. Jakob and T. McNally, 2001: Model clouds over oceans as seen from space: comparison with HIRS/2 and MSU radiances. *J. Climate*, **14,** 4216–4229.

[Chevallier and Kelly, 2002] Chevallier, F. and G. Kelly, 2002: Model Clouds over Oceans as Seen from Space: Comparison with Geostationary Imagery in the 11-μm Window Channel. *Mon. Wea. Rev.*, **130,** 712–722.

[Chepfer *et al.*, 1999] Chepfer, H., J. Pelon, G. Brogniez, C. Flamant, V. Trouillet and P.H. Flamant, 1999: Impact of cirrus cloud ice crystal shape and size on multiple scattering effects: application to spaceborne and airborne backscatter lidar measurements during LITE mission and E LITE campaign. *Geophys. Res. Lett.*, **26,** 2203–2206.

[ESA, 1999] European Space Agency, 1999: The Four Candidate Earth Explorer Core Missions – Atmospheric Dynamics Mission. *ESA Report for Mission Selection*, **ESA SP-1233(4),** 157 pp.

[Fisher, 2003] Fisher, M., 2003: Estimation of entropy reduction and degrees of freedom for signal for large varaitional analysis systems. *ECMWF Tech.Memo.*, **397,** 18 pp.

[Fisher and Andersson, 2001] Fisher, M. and E. Andersson, 2001: Developments in 4D-Var and Kalman Filtering. *ECMWF Tech.Memo.*, **347,** 36 pp.

[Fisher and Courtier, 1995] Fisher, M. and P. Courtier, 1995: Estimating the covariance matrices of analysis and forecast error in variational data assimilation. *ECMWF Tech.Memo.*, **220,** 26 pp.

[Hollingsworth and Lönnberg, 1986] Hollingsworth, A. and P. Lönnberg, 1986: The statistical structure of short-range forecast errors as determined from radiosonde data. Part I: The wind field. *Tellus*, **38A,** 111–136.

[Isaksen and Janssen, submitted] Isaksen, L. and P. A. E. M. Janssen, 2003: Impact of ERS scatterometer winds in ECMWF's assimilation system. *Q. J. R. Meteorol. Soc.*, accepted.

[Jakob and Klein, 2000] Jakob, C. and S.A. Klein, 2000: A parametrization of the effects of cloud and precipitation overlap for use in general-circulation models. *Q. J. R. Meteorol. Soc.*, **126,** 2525–2544.

[Klinker *et al.*, 1998] Klinker, E., F. Rabier and R. Gelaro, 1998: Estimation of key analysis errors using the adjoint technique. *Q. J. R. Meteorol. Soc.*, **124,** 1909–1933.

[Marseille and Bouttier, 2001] Marseille, G. J. and F. Bouttier, 2001: Climatologies of sensitive areas for short-term forecast errors over Europe – EUMETNET-EUCOS study. *ECMWF Tech.Memo.*, **334,** 50 pp.

[Marseille and Stoffelen, 2003] Marseille, G. J. and A. Stoffelen, 2003: Simulation of wind profiles from a spave-borne Doppler wind lidar. *Q. J. R. Meteorol. Soc.*, **129,** 3079–3098.

[Marseille *et al.*, 2001] Marseille, G. J., A. Stoffelen, F. Bouttier, C. Cardinali, S. de Haan and D. Vasiljevic, 2001: Impact assessment of a doppler wind lidar in space on atmospheric analyses and numerical weather prediction. *KNMI Scientific Report*, **WR 2001-03,** 56pp.

[Marseille *et al.*, submitted] Marseille, G. J., A. Stoffelen and A. van Lammeran: A novel method for aerosol backscatter retrieval from LITE data. *J. Geophys. Res.*, Submitted.

[McCormick *et al.*, 1993] McCormick, M. P., D. M. Winker, E. V. Browell, J. A. Coakley, C. S. Gardner, R. M. Hoff, G. S. Kent, S. H. Melfi, R. T. Menzies, C. M. R. Platt, D. A. Randall and J. A. Reagan, 1993: Scientific investigations planned for the Lidar In-Space Technology Experiment (LITE). *Bull. Amer. Meteorol. Soc.*, **74,** 205–214.

[McNally, 2002] McNally, A. P., 2002: A note on the occurrence of cloud in meteorologically sensitive areas and the implications for advanced infrared sounders. *Q. J. R. Meteorol. Soc.*, **128,** 2551–2556.

[Miller *et al.*, 1999] Miller, S. D., G. L. Stephens and A. C. M. Beljaars, 1999: A Validation Survey of the ECMWF Prognostic Cloud Scheme using LITE. *Geophys. Res. Lett.*, **26,** 1417–1420.

[Rabier *et al.*, 1996] Rabier, F., E. Klinker, P. Courtier and A. Hollingsworth, 1996: Sensitivity of forecast errors to initial conditions. *Q. J. R. Meteorol. Soc.*, **122,** 121–150.

[Schmetz *et al.*, 1993] Schmetz, J., K. Holmlund, J. Hoffman, B. Strauss, B. Mason, V. Gaertner, A. Koch and L. van De Berg, 1993: Operational cloud-motion winds from Meteosat infrared images. *J. Appl. Meteorol.*, **32,** 1206–1225.

[Simmons and Hollingsworth, 2002] Simmons, A. and A. Hollingsworth, 2002: Some aspects of the improvement in skill of numerical weather prediction. *Q. J. R. Meteorol. Soc.*, **128,** 647–687.

[Stoffelen and Marseille, 1998] Stoffelen, A. and G. J. Marseille, 1998: Study on the Utility of a Doppler Wind Lidar for Numerical Weather Prediction and Climate. **ESA-CR(P)-4198,** 56pp+apps+figs.

[Stoffelen *et al.*, 2002] Stoffelen, A., M. Håkansson and G. J. Marseille, 2002: Measurement Error and Correlation Impact on the Atmospheric Dynamics Mission: Report on Tasks 3 and 4. *Study Report*, ESA Contract **RFQ/3-9992/01/NL/MM,** 75pp.

[Stoffelen *et al.*, submitted] Stoffelen, A., J. Pailleux, E. Källén, J. M. Vaughan, L. Isaksen, P. Flamant, W. Wergen, E. Andersson, H. Schyberg, A. Culoma, R. Meynart, M. Endemann and P. Ingmann, 2003: The atmospheric dynamics mission for global wind measurement. *Bull. Amer. Meteorol. Soc.*, Submitted.

[Thépaut and Andersson, 2003] Thépaut, J.-N. and E. Andersson, 2003: Assimilation of high-resolution satellite data. *ECMWF Newsletter*, **97,** 6–11.

[Uppala, 1997] Uppala, S., 1997: Observing System Performance in ERA. *ECMWF Re-Analysis Final Report Series*, **3,** 261pp.

[Vaughan *et al.*, 1995] Vaughan, J. M., D. W. Brown, C. Nash, S. B. Alejandro and G. G. Koenig, 1995: Atlantic atmospheric aerosol studies 2. Compendium of airborne backscatter measurements at 10.6 μm. *J. Geophys. Res.*, **100**(D1), 1043–1065.

[Veldman *et al.*, 1999] Veldman, S. M., H. A. Knobbout, A. Stoffelen, G. J. Marseille and E. A. Kuijpers, 1999: Lidar Performance Analysis Simulator (LIPAS). Part 8: Summary. *Study Report*, ESA Contract **12718/98/NL/GD,** 50pp.

[Winker and Vaughan, 1994] Winker, D. M. and M. A. Vaughan, 1994: Vertical distribution of clouds over Hampton, Virginia observed by lidar under the ECLIPS and FIRE ETO programs. *Atmos. Res.*, **34,** 117–133.

[Winker *et al.*, 1996] Winker, D. M., R. H. Couch and M. P. McCormick, 1996: An overview of LITE: NASA's Lidar in-space Technology Experiment. *Proc. IEEE*, **84,** 164–180.

[WMO, 2001] World Meteorological Organization, 2001: Statement of Guidance regarding how well Satellite and In Situ Sensor Capabilities meet WMO User Requirements in Several Application Areas. *WMO Satellite Reports SAT-26*, **WMO/TD No. 1052,** 9-13.

[Žagar *et al.*, submitted] Žagar, N., N. Gustafsson and E. Källén, 2003: Variational data assimilation in the tropics: the impact of background error constraint. *Q. J. R. Meteorol. Soc.*, submitted.

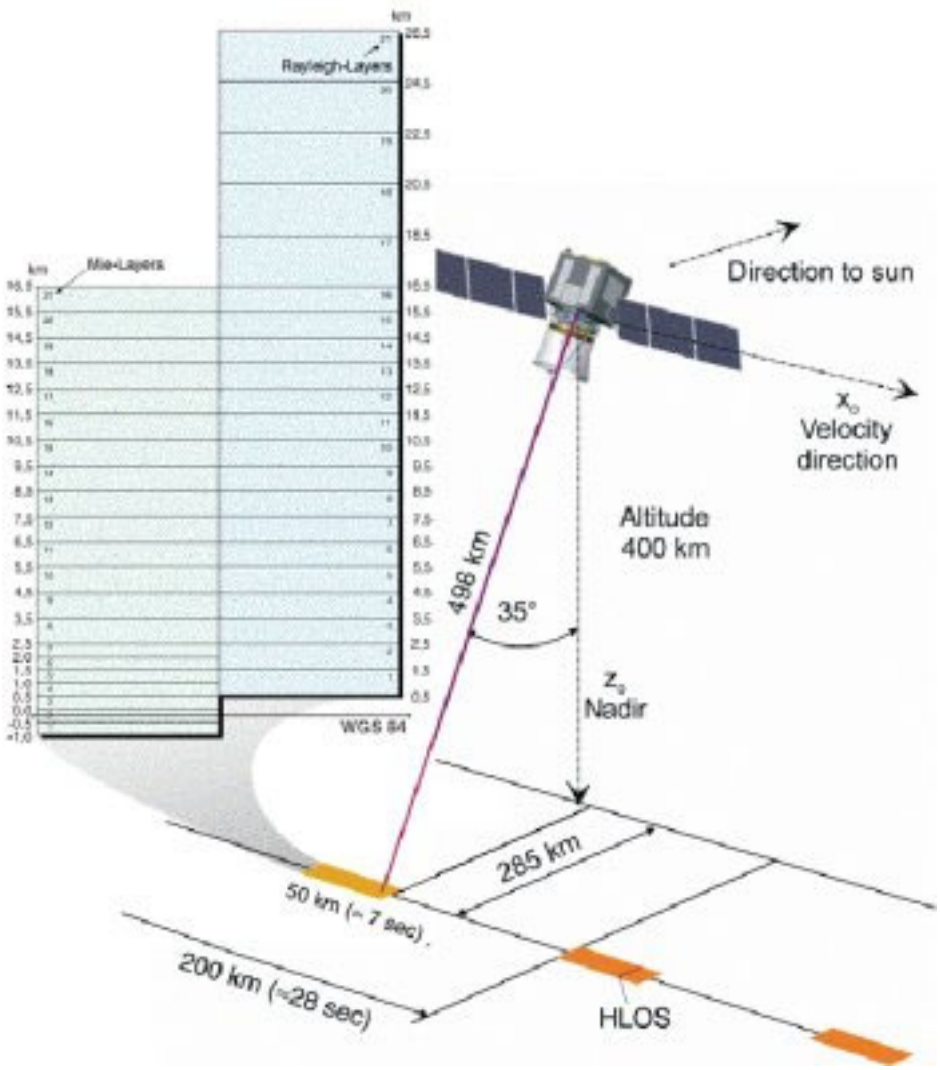

Figure 1: Vertical resolution and viewing geometry of the Aeolus instrument. (Source: ESA website http://www.esa.int)

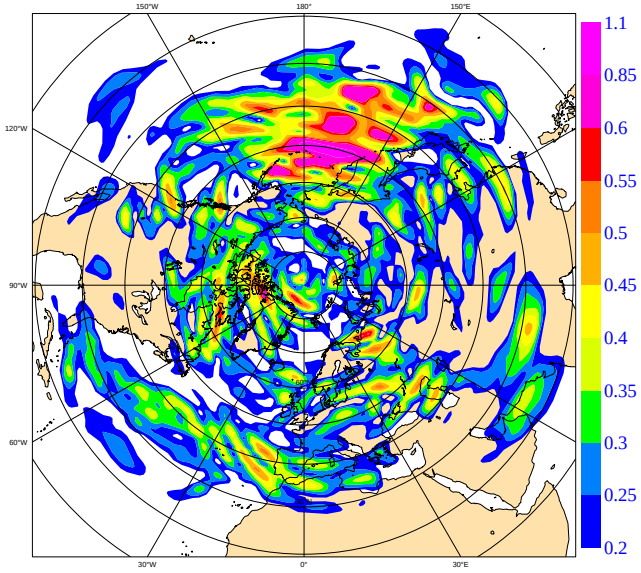

Figure 2: Key analysis error, zonal wind in ms^{-1}, rms for the period 9–16 September 1994. The model level shown is close to 250 hPa. Values less than 0.2 ms^{-1} are left unshaded.

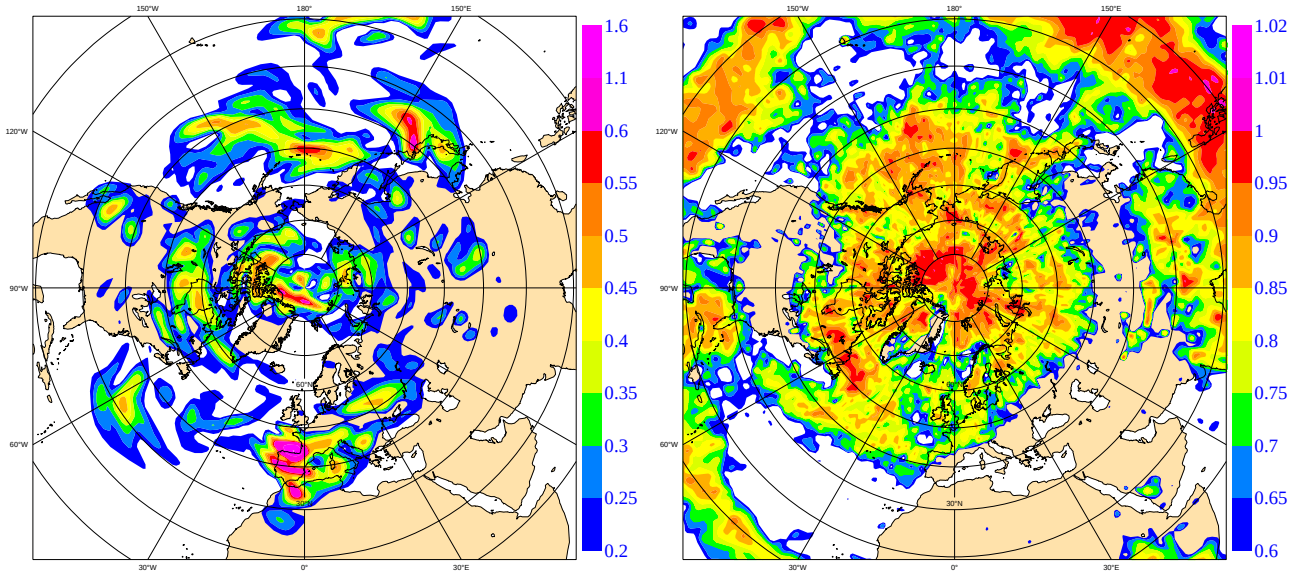

Figure 3: Key analysis error, zonal wind at 850 hPa (left panel) shaded between 0.2 and 1.6 ms^{-1} (see legend) and rms of total cloud cover (right panel) shaded between 0.6 and 1. (see legend)

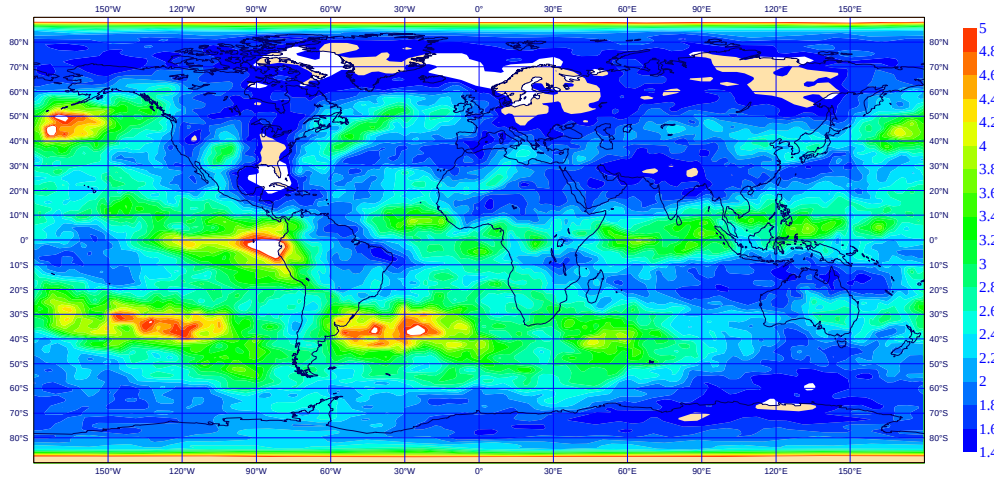

Figure 4: Accuracy of zonal wind (in ms^{-1}) at 250 hPa estimated with a data assimilation ensemble, October 2000. The spread between 12-hour forecasts is indicative of background error for the ECMWF data assimilation system (version 23r4 used Autumn 2001). Shading between 1.4 and 5 ms^{-1} (see legend).

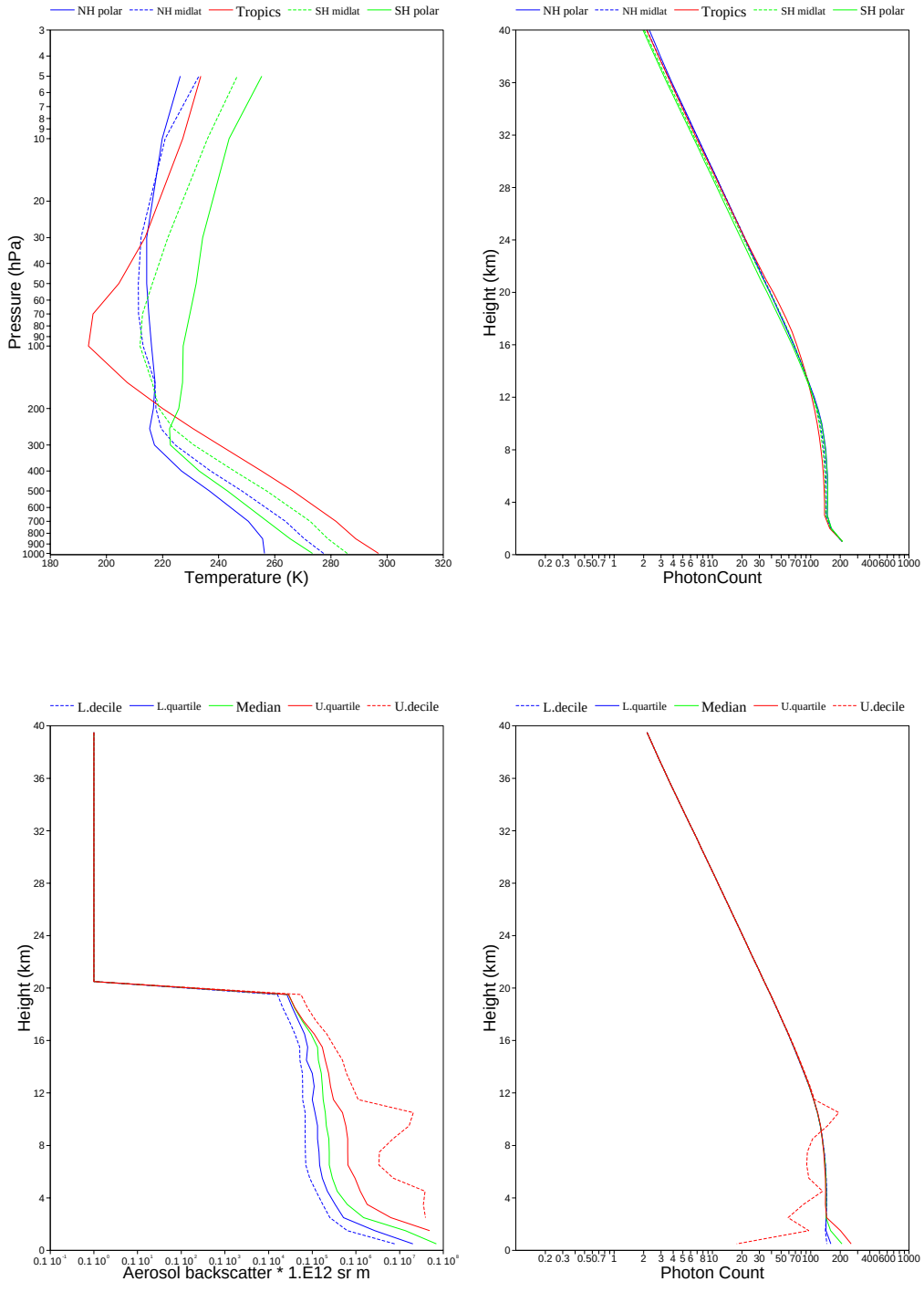

Figure 5: Input profiles for temperature (upper left) and aerosol backscatter (lower left) and corresponding photon counts (right panels).

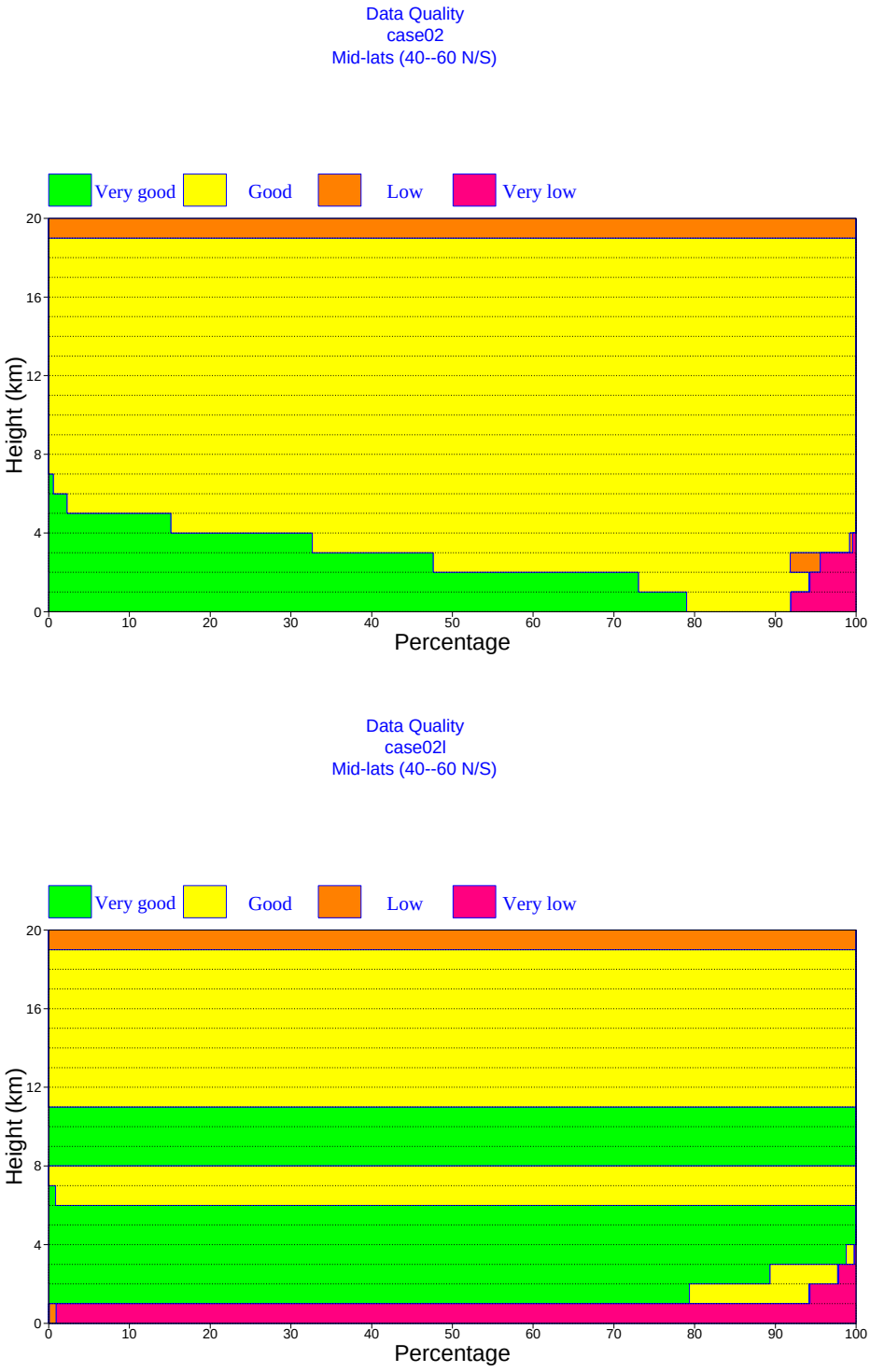

Figure 6: Statistics of DWL observation quality in 4 classes labeled very good, good, low and very low (see legend). 1400 observations have been simulated with median backscatter (upper panel) and upper decile backscatter (lower panel).

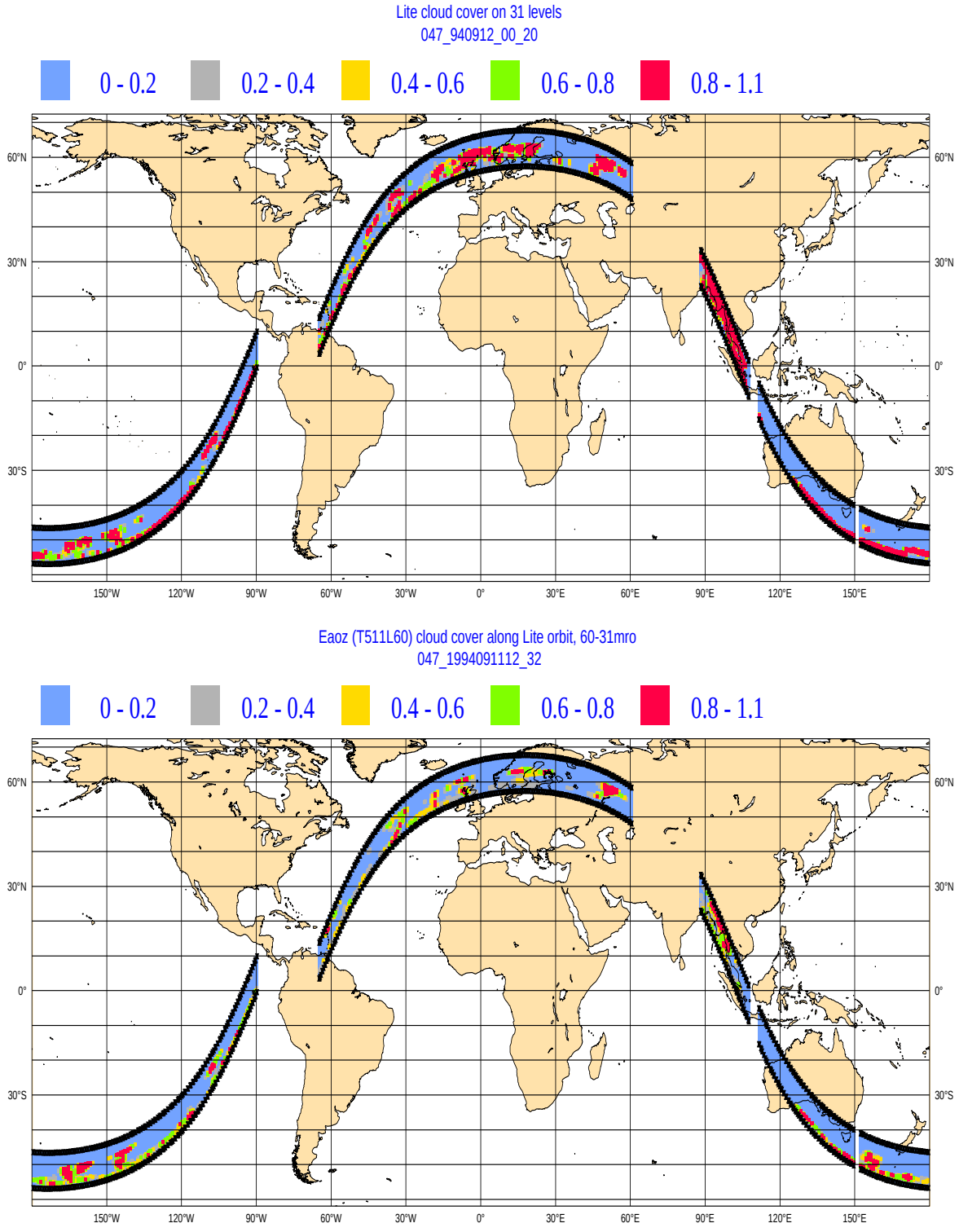

Figure 7: Profiles of cloud cover (see legend) along LITE orbit 047 (12 Sep. 1994) from LITE retrievals (upper panel) and the ECMWF model (lower panel). The lower black curve is the satellite track, the upper black curve is approximately 10 hPa. The vertical scale in the boundary layer is exaggerated.

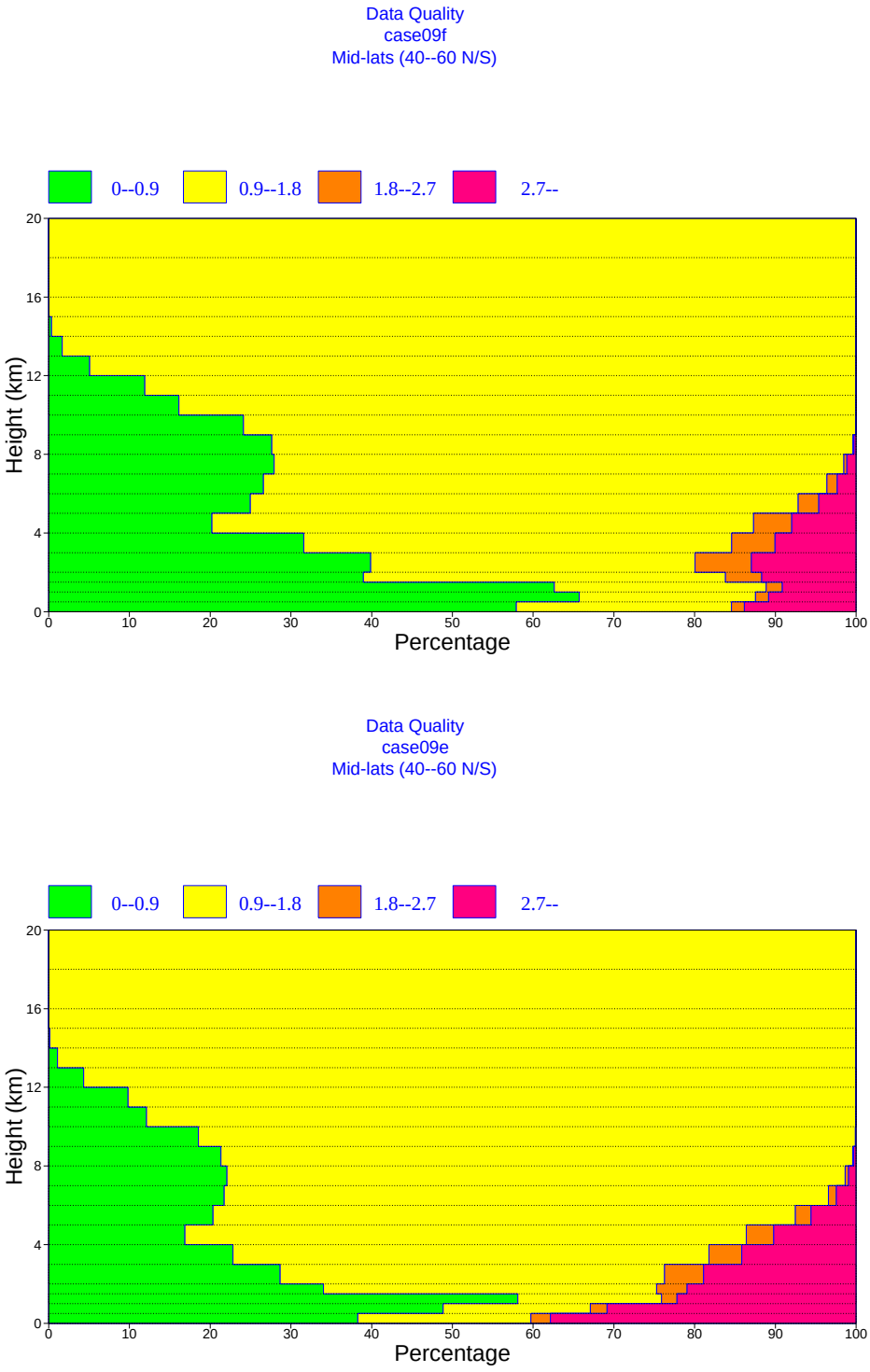

Figure 8: Statistics of DWL observation quality (defined in text) for the LITE period. 5633 mid-latitude observations have been simulated with ECMWF model cloud cover (upper panel) and LITE-inferred cloud cover (lower panel).

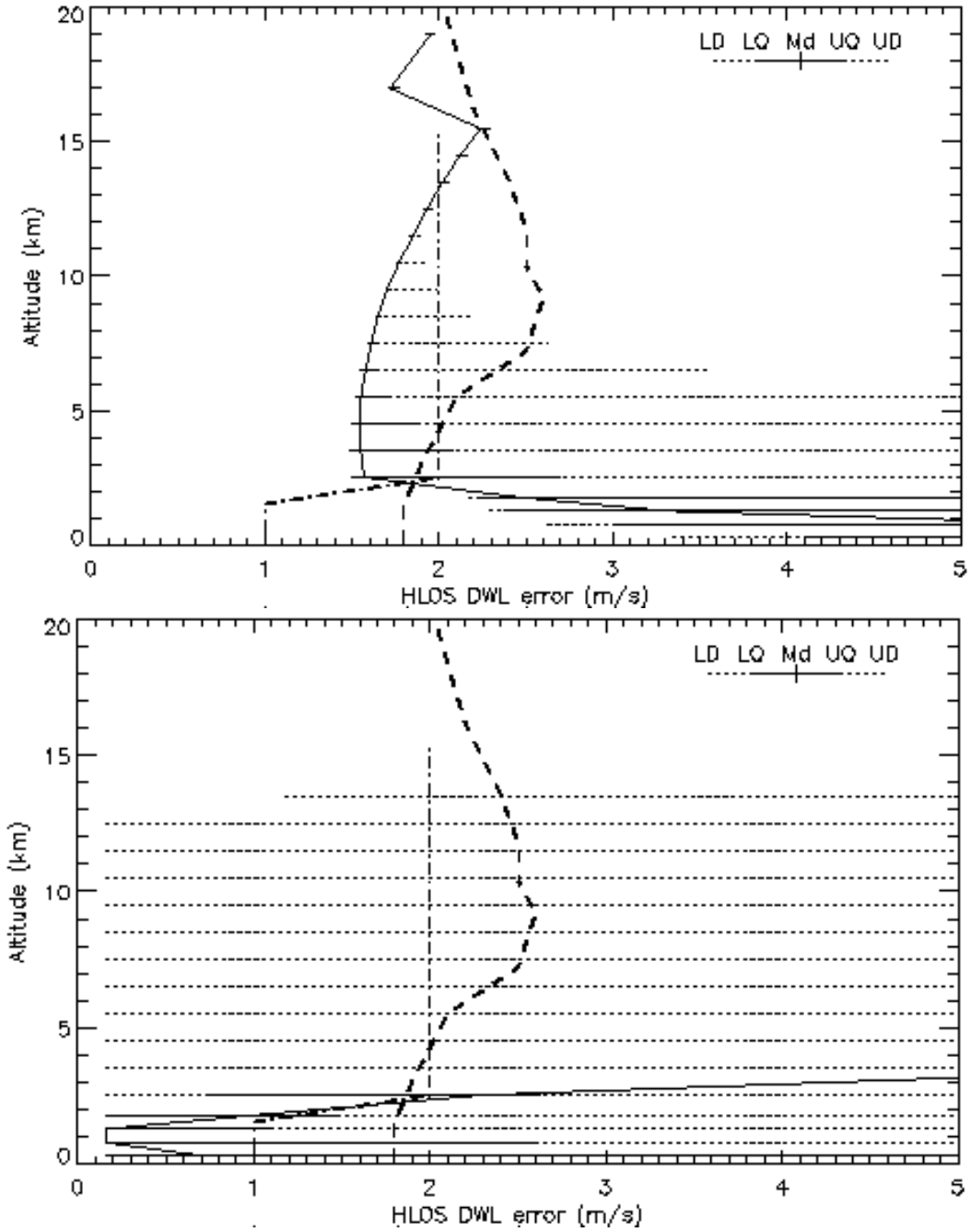

Figure 9: Distribution of simulated Aeolus instrument random error (in ms^{-1}) using LITE-inferred cloud cover. The median is shown as a profile (full line) with the spread indicated with horizontal lines spanning the lower and upper quartiles (full lines) and deciles (dotted). Radiosonde errors (thick dashed) and the ADM-Aeolus instrument specification (dash-dotted) are also shown. The two panels show Rayleigh channel ($\hat{\sigma}_R$) (upper) and Mie channel ($\hat{\sigma}_M$) (lower).

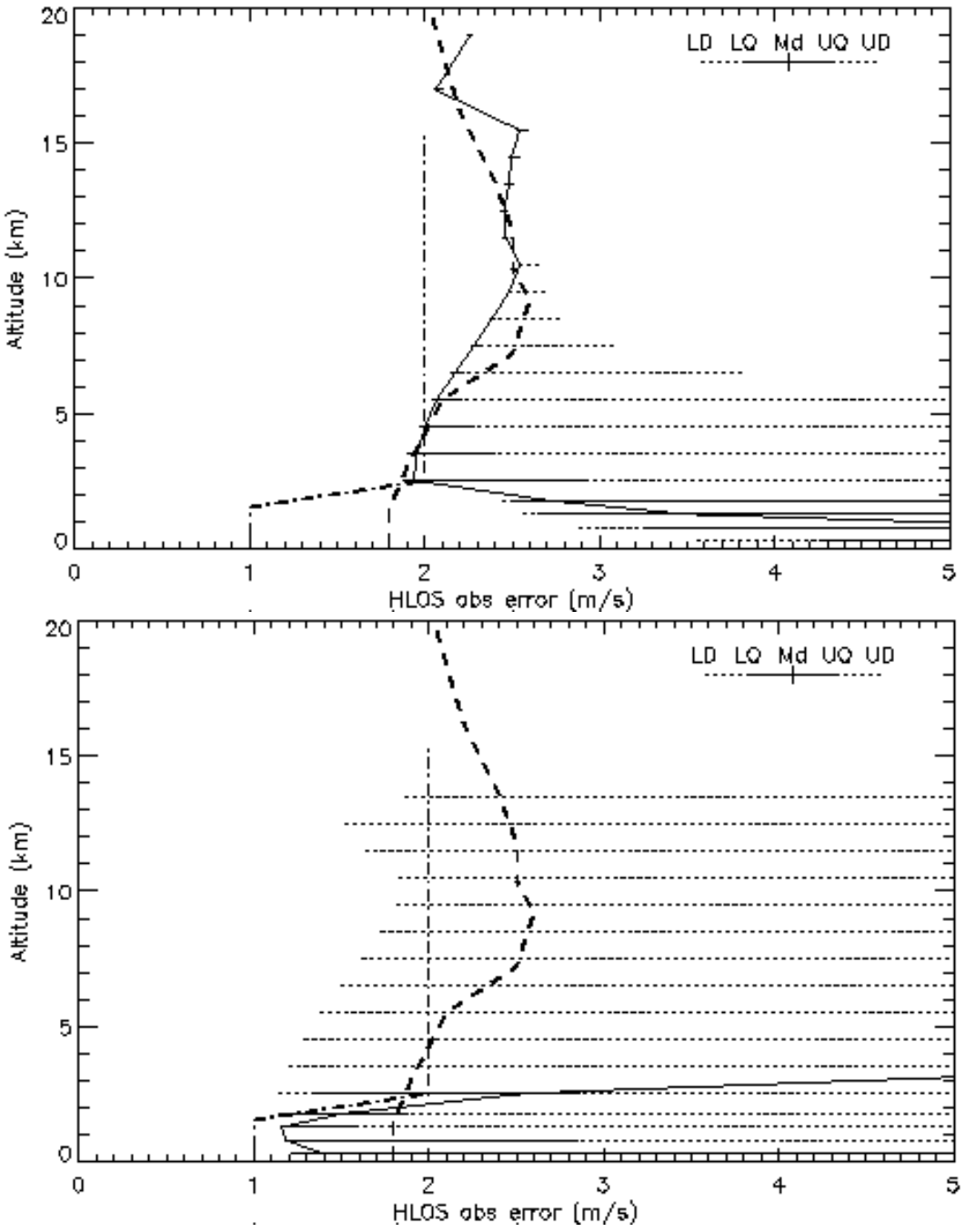

Figure 10: Like Fig. 9 but for observation random error (in ms^{-1}).

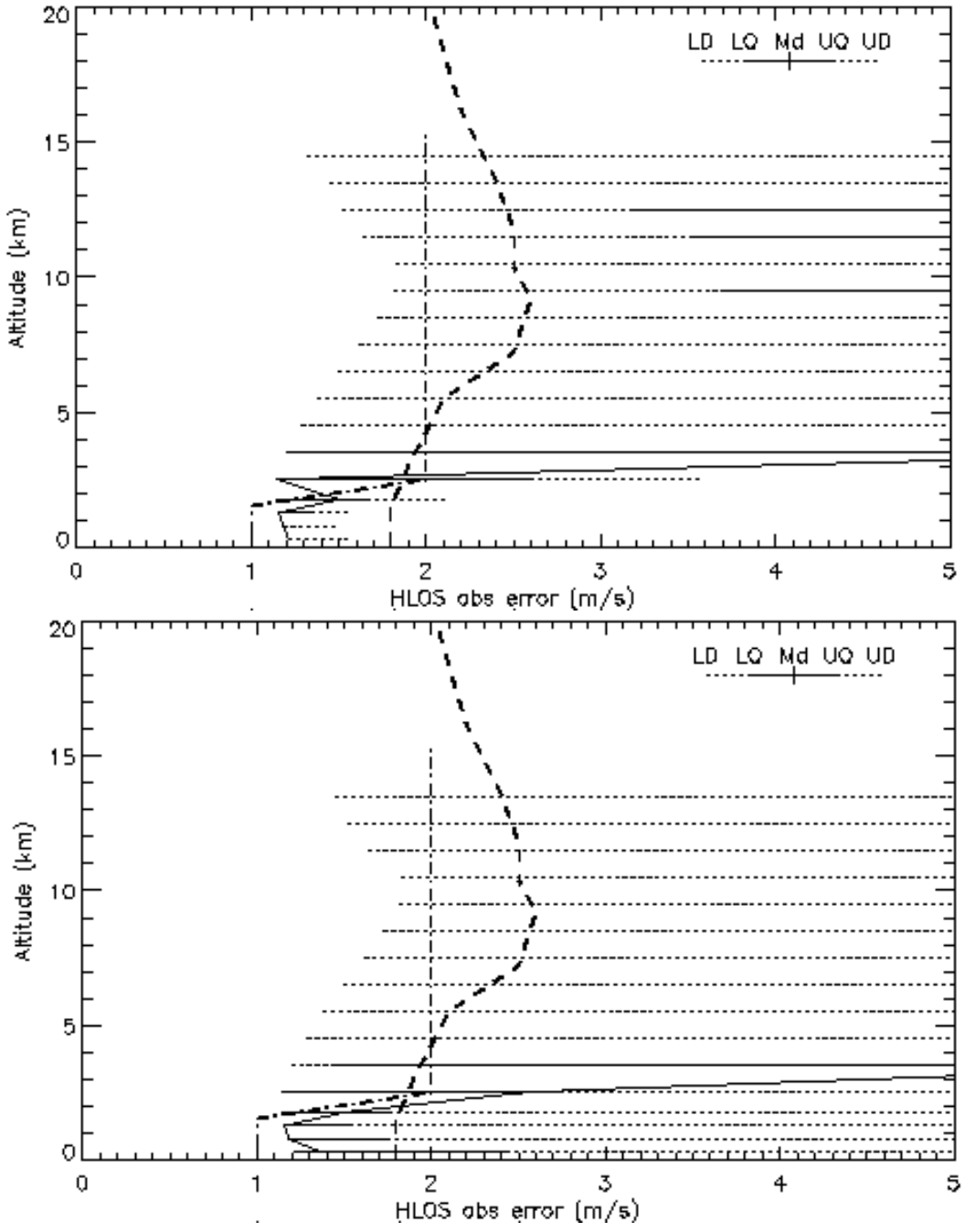

Figure 11: Distribution of simulated Aeolus observation random error, Mie channel (σ_M, ms^{-1}), North Atlantic. Upper panel: using model cloud cover, lower panel: using LITE-inferred cloud cover. Otherwise like Fig. 9.

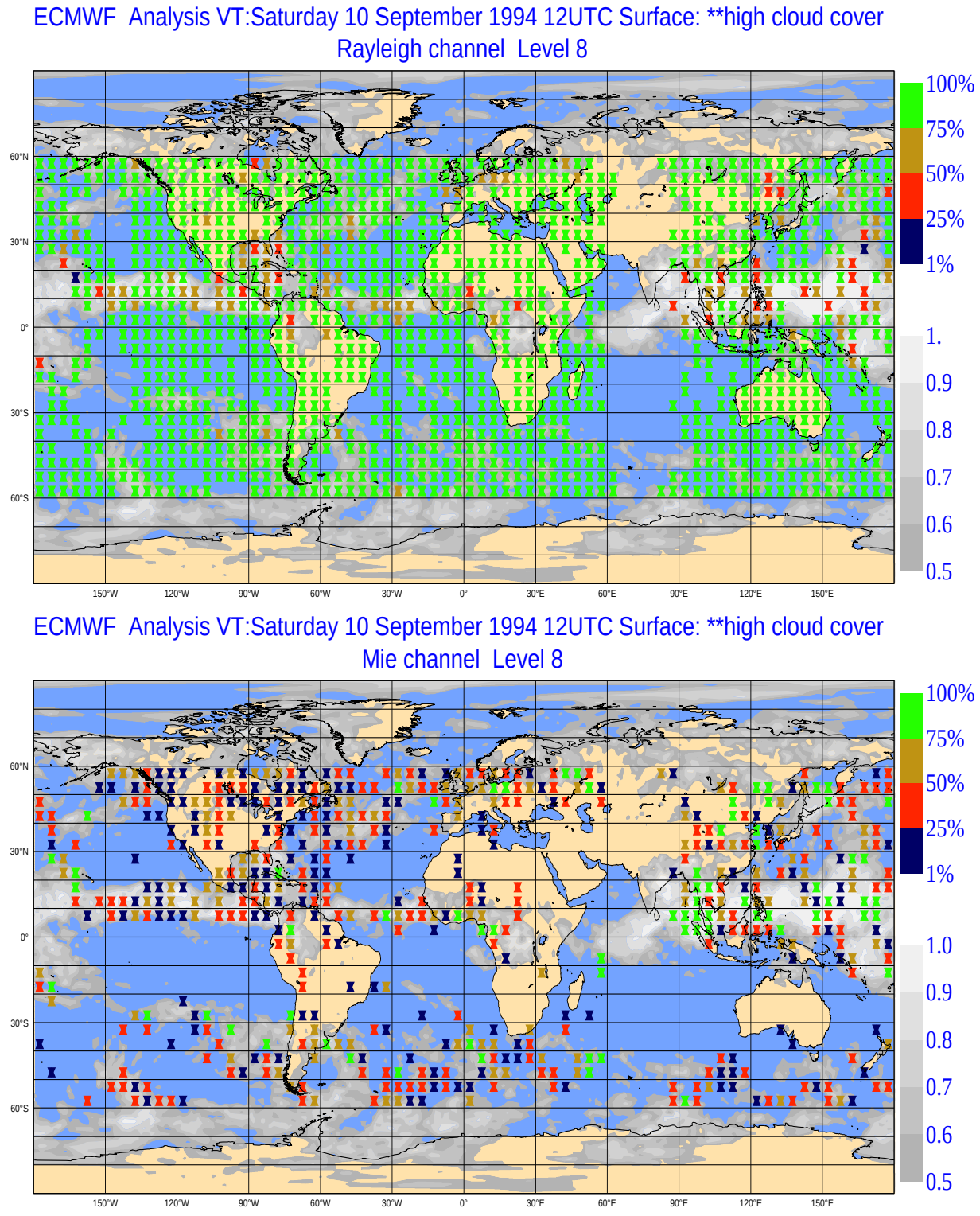

Figure 12: Simulated Aeolus yield at 9–10 km in terms of percentage of good data in 5x5 degree boxes represented by coloured markers (see legend), based on simulations of all available LITE orbits, for Rayleigh channel (upper) and Mie channel (lower). Shading shows rms of ECMWF high cloud cover within the LITE period.

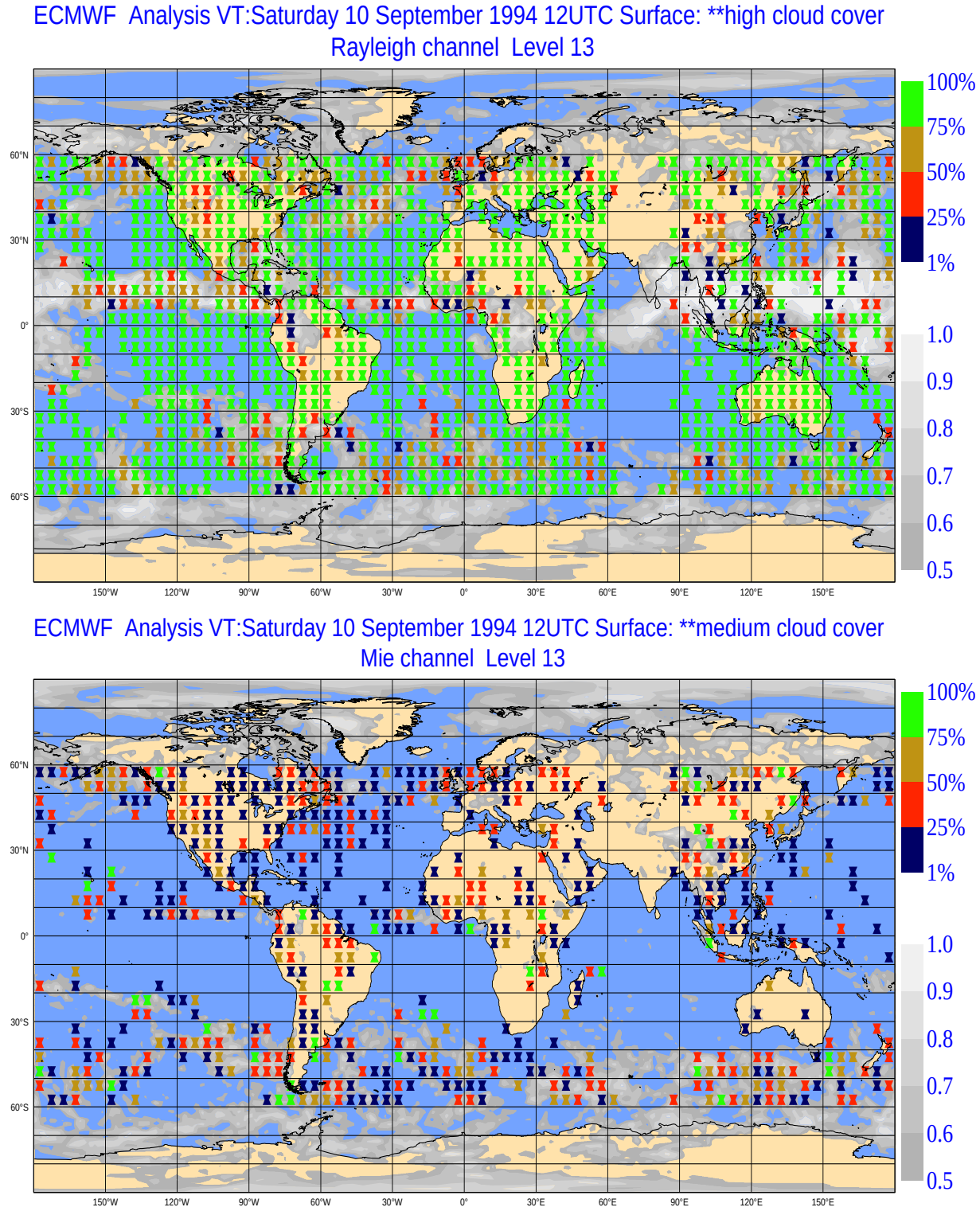

Figure 13: Simulated Aeolus yield at 4–5 km. Upper: Rayleigh channel/high cloud cover, lower: Mie channel/medium cloud cover. Otherwise like Fig. 12

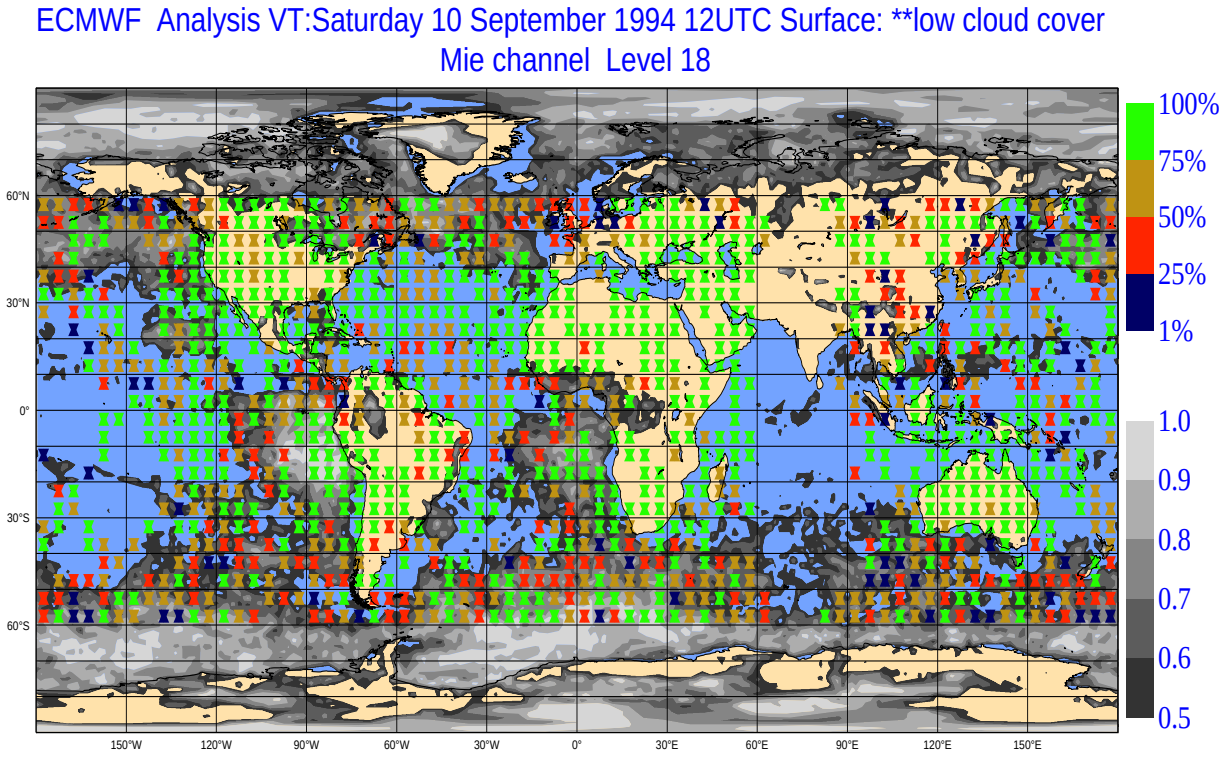

Figure 14: Simulated Aeolus yield at 0.5–1 km for Mie channel. Shading shows rms of ECMWF low cloud cover. Otherwise like Fig. 12